

PROPERTIES OF A PARTIALLY COHERENT SINE BEAM IN NON-KOLMOGOROV TURBULENCE

Peiyong Zhu, Guiqiu Wang, Yan Yin, Haiyang Zhong, Yaochuan Wang, and Dajun Liu*

*Department of Physics, Dalian Maritime University
Dalian 116026, China*

*Corresponding author e-mail: liudajun@dlnu.edu.cn

Abstract

We present the expression of a partially coherent sine beam and derive the propagation equations of such a beam in non-Kolmogorov turbulence. The intensity profiles of the beam in non-Kolmogorov turbulence are simulated and analyzed. The obtained results show that the sinusoidal array profile is destroyed by non-Kolmogorov turbulence and beam parameters during the propagation, and the intensity profile of such a beam becomes a sheet, when a and b are set. The array profile properties of partially coherent sine beams introduced here display new properties, and these beams help free space optical communications.

Keywords: sine beam, intensity, atmospheric turbulence, partially coherent beam.

1. Introduction

The influences of turbulent environments on light properties are widely studied owing to the demands of free space optical (FSO) communications and laser sensing. Analysis of the average intensity of various coherent beams in the atmosphere [1–5] has found that the intensity profile becomes Gaussian during the propagation. A partially coherent beam (PCB) is resistant to the harmful effects of turbulence, and the evolutions of PCBs in turbulence have been extensively studied [6–10]. The shape of PCBs can be modulated with a spatial coherence function [11], and these beams can overcome the harmful effects of complex environments. The PCB properties correlated with the special coherence function have been widely analyzed [12–20], and it has been found that the coherence function influenced on the PCB evolutions. It is known that a beam array can provide higher power. In studies on models of beam arrays and their propagation in turbulence [21–30], it has been found that a beam array can evolve into a Gaussian beam during the propagation. The propagation of a vortex PCB in vertical turbulent links has been analyzed and found to be suitable for FSO communications [31]. PCBs with flat-topped shapes can achieve better fiber-coupling efficiency in FSO communications [32]. Recently, a new beam with a sinusoidal profile was introduced, and the properties of a sine beam in a uniaxial crystal were studied [33]. It will be interesting to view the interaction of sine beams with turbulence. In this paper, we introduce the equation of a partially coherent sine (PC-sin) beam correlated with a Gaussian–Schell model (GSM) source. The cross-spectral density (CSD) of the PC-sin beam in non-Kolmogorov turbulence is derived. The intensity profiles of such beams propagating in non-Kolmogorov turbulence are analyzed in detail.

2. Theory

The field of a sine beam is expressed as [33]

$$U(r) = \sin(ax) \sin(by), \tag{1}$$

where a and b represent displacement parameters. Considering a PCB correlated with a GSM correlator [34–36], the CSD of a PC-sin beam generated by a GSM source can be written as follows:

$$\Gamma(r_1, r_2, z = 0) = \sin(ax_1) \sin(by_1) \sin(ax_2) \sin(by_2) \exp \left[-\frac{(x_2 - x_1)^2 + (y_2 - y_1)^2}{2\sigma_0^2} \right], \tag{2}$$

where σ_0 is the coherence length.

The CSD of the PC-sin beam propagating in turbulence can be described by the extended Huygens–Fresnel principle [1, 10],

$$\Gamma(\rho_1, \rho_2, L) = \frac{k^2}{4\pi^2 z^2} \int_{-\infty}^{+\infty} \int_{-\infty}^{+\infty} \int_{-\infty}^{+\infty} \int_{-\infty}^{+\infty} \Gamma(r_1, r_2, 0) \exp \left[-\frac{ik}{2z}(\rho_1 - r_1)^2 + \frac{ik}{2z}(\rho_2 - r_2)^2 \right] \times \langle \exp[\psi(r_1, \rho_1) + \psi^*(r_2, \rho_2)] \rangle dr_1 dr_2, \tag{3}$$

with

$$\langle \exp[\psi(r_1, \rho_1) + \psi^*(r_2, \rho_2)] \rangle = \exp \left[-\frac{(r_1 - r_2)^2 + (r_1 - r_2)(\rho_1 - \rho_2) + (\rho_1 - \rho_2)^2}{T_0^2} \right]. \tag{4}$$

Let T_0 be the coherence length in non-Kolmogorov turbulence; it is given by [12, 14]

$$\frac{1}{T_0^2} = \frac{\pi^2 k^2 z}{6(\alpha - 2)} A(\alpha) C_n^2 \left[(2\kappa_0^2 - 2\kappa_m^2 + \alpha\kappa_m^2) \kappa_m^{2-\alpha} \exp \left(\frac{\kappa_0^2}{\kappa_m^2} \right) \Gamma \left(2 - \frac{\alpha}{2}, \frac{\kappa_0^2}{\kappa_m^2} \right) - 2\kappa_0^{4-\alpha} \right], \tag{5}$$

$$A(\alpha) = \frac{1}{4\pi^2} \Gamma(\alpha - 1) \cos \left(\frac{\alpha\pi}{2} \right), \tag{6}$$

$$c(\alpha) = \left[\frac{2\pi}{3} \Gamma \left(\frac{5 - \alpha}{2} \right) A(\alpha) \right]^{1/(\alpha-5)}, \tag{7}$$

where α is the power-law constant, C_n^2 is the structure constant, $\kappa_0 = 2\pi/L_0$ with L_0 being the outer scale, and $\kappa_m = c(\alpha)/l_0$ with l_0 being the inner scale. After substituting Eqs. (2) and (4) into Eq. (3), we obtain the CSD of the PC-sin beam at L ; it reads

$$\Gamma(\rho_1, \rho_2, L) = \frac{k^2}{4\pi^2 z^2} \frac{1}{2^4} \exp \left[-\frac{ik}{2z}(\rho_1^2 - \rho_2^2) \right] \exp \left[-\frac{(\rho_{1x} - \rho_{2x})^2 + (\rho_{1y} - \rho_{2y})^2}{T_0^2} \right] \times (M_{++} - M_{x+-} - M_{x-+} + M_{x--})(N_{++} - N_{+-} - N_{-+} + N_{--}), \tag{8}$$

where

$$M_{\pm\pm} = \sqrt{\frac{\pi}{p}} \exp \left[\frac{1}{p} \left(\pm \frac{ia}{2} + \frac{ik}{2L} \rho_{1x} - \frac{\rho_{1x} - \rho_{2x}}{2T_0^2} \right)^2 \right] \sqrt{\frac{\pi}{q}} \exp \left(\frac{X_{\pm\pm}^2}{q} \right), \tag{9}$$

$$N_{\pm\pm} = \sqrt{\frac{\pi}{p}} \exp \left[\frac{1}{p} \left(\pm \frac{ib}{2} + \frac{ik}{2L} \rho_{1y} - \frac{\rho_{1y} - \rho_{2y}}{2T_0^2} \right)^2 \right] \sqrt{\frac{\pi}{q}} \exp \left(\frac{Y_{\pm\pm}^2}{q} \right), \tag{10}$$

with

$$p = \frac{1}{2\sigma_0^2} + \frac{1}{T_0^2} + \frac{ik}{2L}, \quad (11)$$

$$q = \frac{1}{2\sigma_0^2} + \frac{1}{\rho_0^2} - \frac{ik}{2L} - \frac{1}{p} \left(\frac{1}{2\sigma_0^2} + \frac{1}{T_0^2} \right)^2, \quad (12)$$

$$X_{+\pm} = \pm \frac{ia}{2} - \frac{ik}{2L} \rho_{2x} + \frac{\rho_{1x} - \rho_{2x}}{2T_0^2} + \frac{1}{p} \left(\frac{1}{2\sigma_0^2} + \frac{1}{T_0^2} \right) \left(\frac{ia}{2} + \frac{ik}{2L} \rho_{1x} - \frac{\rho_{1x} - \rho_{2x}}{2T_0^2} \right), \quad (13)$$

$$X_{-\pm} = \pm \frac{ia}{2} - \frac{ik}{2L} \rho_{2x} + \frac{\rho_{1x} - \rho_{2x}}{2T_0^2} + \frac{1}{p} \left(\frac{1}{2\sigma_0^2} + \frac{1}{T_0^2} \right) \left(-\frac{ia}{2} + \frac{ik}{2L} \rho_{1x} - \frac{\rho_{1x} - \rho_{2x}}{2T_0^2} \right), \quad (14)$$

$$Y_{+\pm} = \pm \frac{ib}{2} - \frac{ik}{2L} \rho_{2y} + \frac{\rho_{1y} - \rho_{2y}}{2T_0^2} + \frac{1}{p} \left(\frac{1}{2\sigma_0^2} + \frac{1}{T_0^2} \right) \left(\frac{ib}{2} + \frac{ik}{2L} \rho_{1y} - \frac{\rho_{1y} - \rho_{2y}}{2T_0^2} \right), \quad (15)$$

$$Y_{-\pm} = \pm \frac{ib}{2} - \frac{ik}{2L} \rho_{2y} + \frac{\rho_{1y} - \rho_{2y}}{2T_0^2} + \frac{1}{p} \left(\frac{1}{2\sigma_0^2} + \frac{1}{T_0^2} \right) \left(-\frac{ib}{2} + \frac{ik}{2L} \rho_{1y} - \frac{\rho_{1y} - \rho_{2y}}{2T_0^2} \right). \quad (16)$$

When $\rho_1 = \rho_2 = \rho$ is inserted into Eqs. (8)–(16), the intensity of the PC-sin beam is

$$S(\rho, L) = \Gamma(\rho, \rho, L). \quad (17)$$

3. Results and Analysis

Here, we study the intensity of the PC-sin beam propagating in non-Kolmogorov turbulence. The calculation parameters are set as $\lambda = 1064$ nm, $\alpha = 3.5$, $L_0 = 20$ m, and $l_0 = 1$ mm. In Fig. 1, we illustrate the intensity profiles of PCBs with $a = b = 20$ and $\sigma_0 = 3$ mm propagating in non-Kolmogorov

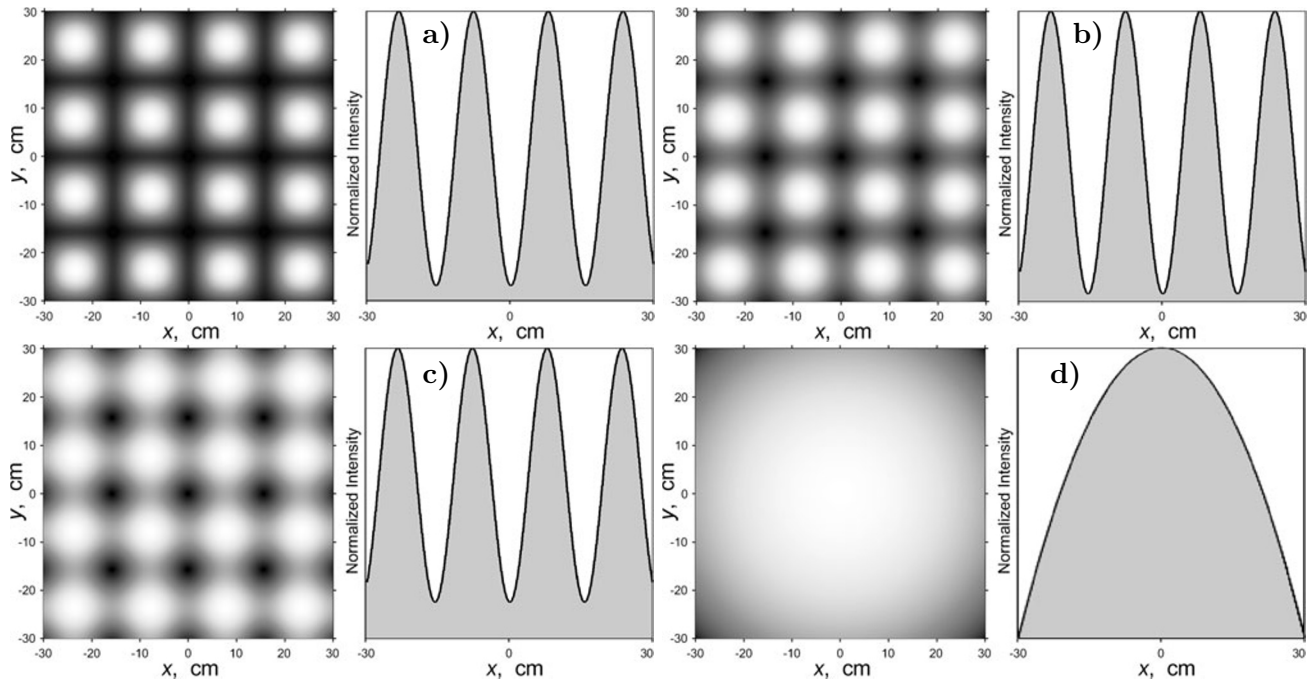


Fig. 1. Normalized intensity of a PC-sin beam with $\sigma_0 = 3$ mm in non-Kolmogorov turbulence. Here, $L = 200$ m (a), $L = 500$ m (b), $L = 1000$ m (c), and $L = 5000$ m (d).

turbulence ($C_n^2 = 10^{-14} \text{ m}^{3-\alpha}$). We find that the intensity profile of the PC-sin beam remains a sinusoidal array profile at $L = 200 \text{ m}$; see Fig. 1 a, and the cross section (with y set at the position of maximum intensity) of the intensity distribution along the x axis shows the sine profile. The beamlets of the PC-sin beam spread and overlap as L increases. At a longer distance $L = 5000 \text{ m}$, the intensity profile of the PC-sin beam evolves from the array profile into a Gaussian profile. The intensity profile of the array beam propagating in turbulence becomes the Gaussian shape owing to the influences of turbulence [26, 37–39].

The average intensity profile of a coherent sine beam ($\sigma_0 = \text{inf}$) propagating in non-Kolmogorov turbulence is shown in Fig. 2 for the same parameters as in Fig. 1. Comparing Fig. 1 c with Fig. 2 a, one can see that the phenomenon that the overlap between the beamlets of coherent sine beam is not more obvious as in the case of PC-sin beam at the same L . By comparing Fig. 1 d with Fig. 2 b, one can see that a sine beam in non-Kolmogorov turbulence remains a sinusoidal array profile.

To show the influences of non-Kolmogorov turbulence and coherence length σ_0 , we present in Fig. 3 the intensity profile of the sine beam through free space. One finds that the array profile of the sine

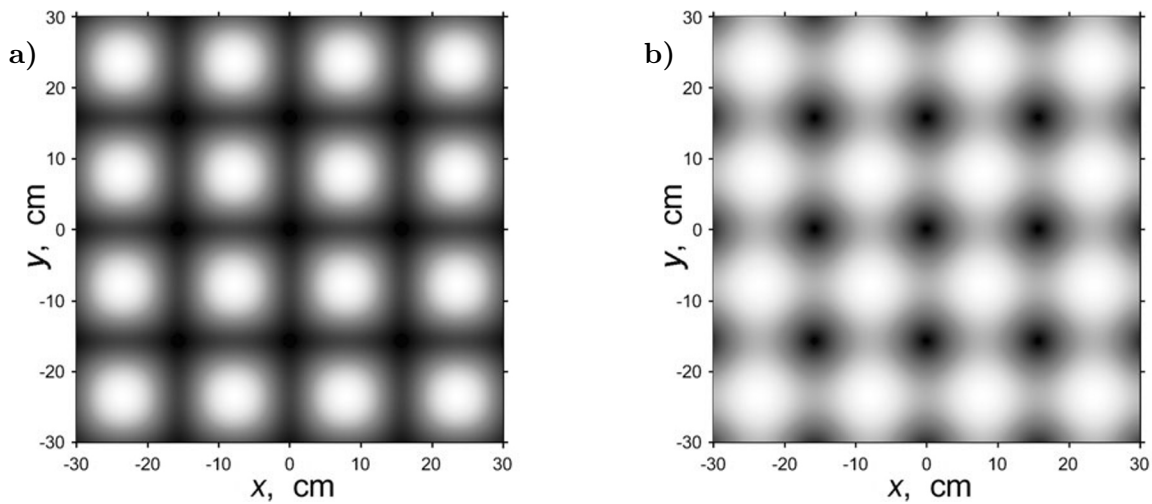


Fig. 2. Normalized intensity of a sine beam in non-Kolmogorov turbulence. Here, $L = 1000 \text{ m}$ (a) and $L = 5000 \text{ m}$ (b).

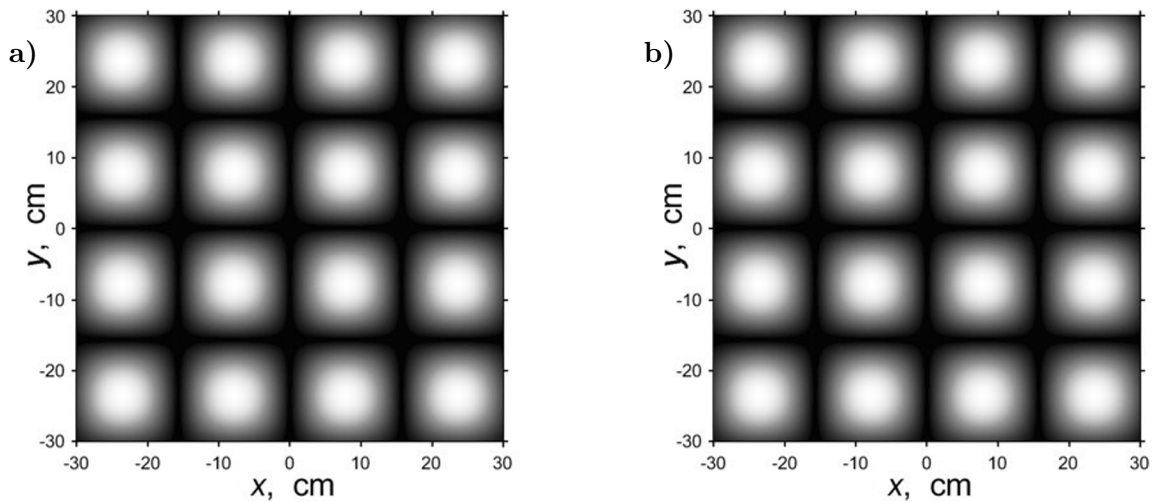


Fig. 3. Normalized intensity of a sine beam in free space. Here, $L = 1000 \text{ m}$ (a) and $L = 5000 \text{ m}$ (b).

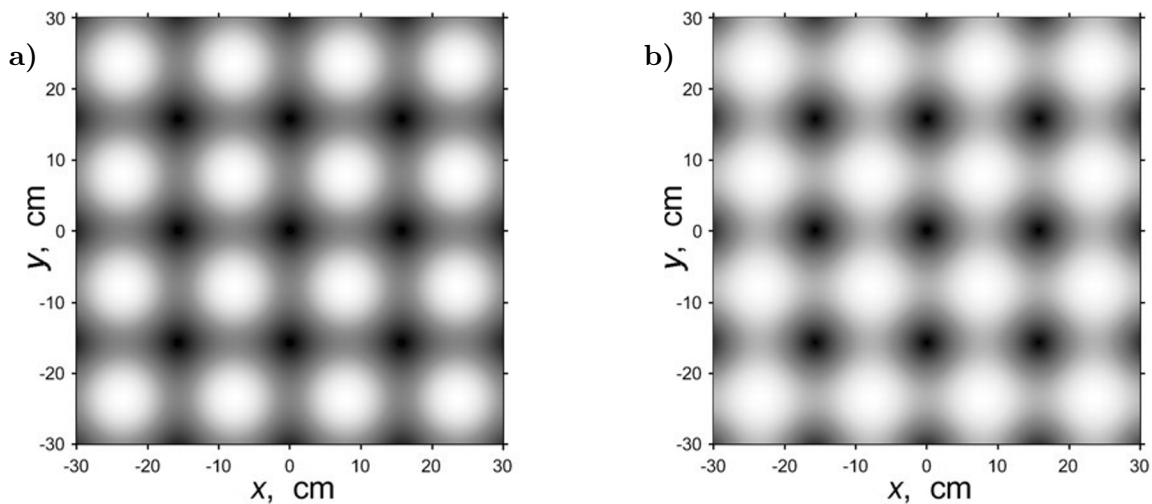


Fig. 4. Normalized intensity of a PC-sin beam with $\sigma_0 = 1$ mm in non-Kolmogorov turbulence. Here, $L = 200$ m (a) and $L = 1000$ m (b).

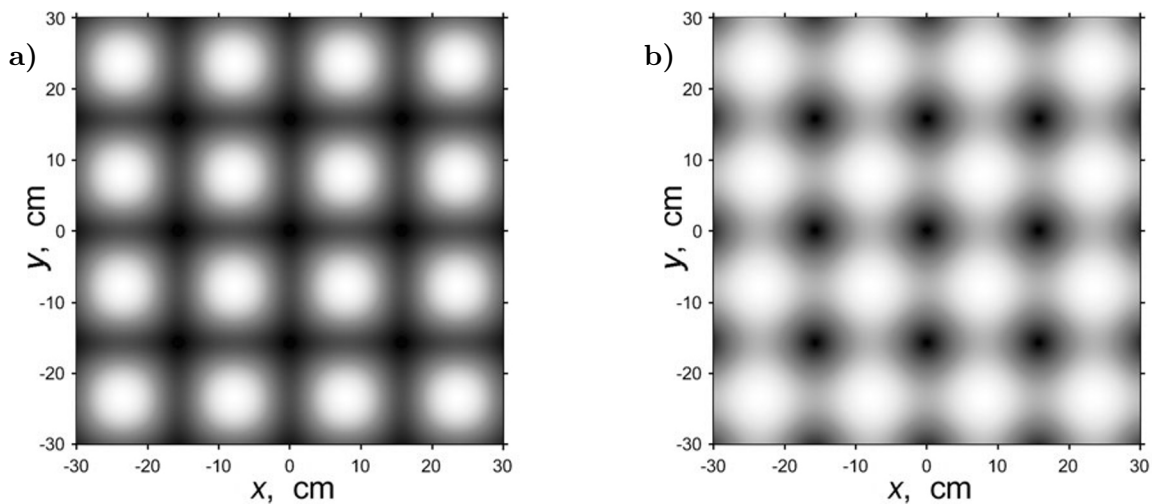


Fig. 5. Normalized intensity of PC-sin beam with $\sigma_0 = 1$ mm in non-Kolmogorov turbulence with $C_n^2 = 10^{-12} \text{ m}^{3-\alpha}$. Here, $L = 200$ m (a) and $L = 1000$ m (b).

beam remains sinusoidal as L increases. From results presented in Figs. 1–3, one can conclude that σ_0 and non-Kolmogorov turbulence destroy the array profile of such a beam during the propagation.

In Fig. 4, we present the intensity profile of the PC-sin beam ($\sigma_0 = 1$ mm) in non-Kolmogorov turbulence. By comparing Fig. 1 a with Fig. 4 a, one can see that the PC-sin beam with a larger σ_0 has a sinusoidal array profile; see Fig. 1 a, and the beamlets of the PC-sin beam with a smaller σ_0 overlap for short L . As L increases, the PC-sin beam with smaller σ_0 will lose the sinusoidal array profile faster. Therefore, the sinusoidal array profile of a beam will be destroyed more quickly, when σ_0 is smaller.

By comparing Fig. 1 with Fig. 5, one can see that, for a PC-sin beam being transmitted in stronger non-Kolmogorov turbulence ($C_n^2 = 10^{-12} \text{ m}^{3-\alpha}$), the sinusoidal array profile overlaps faster. From results presented in Figs. 5 and 6, one can conclude that the sinusoidal array profile of a beam is destroyed more

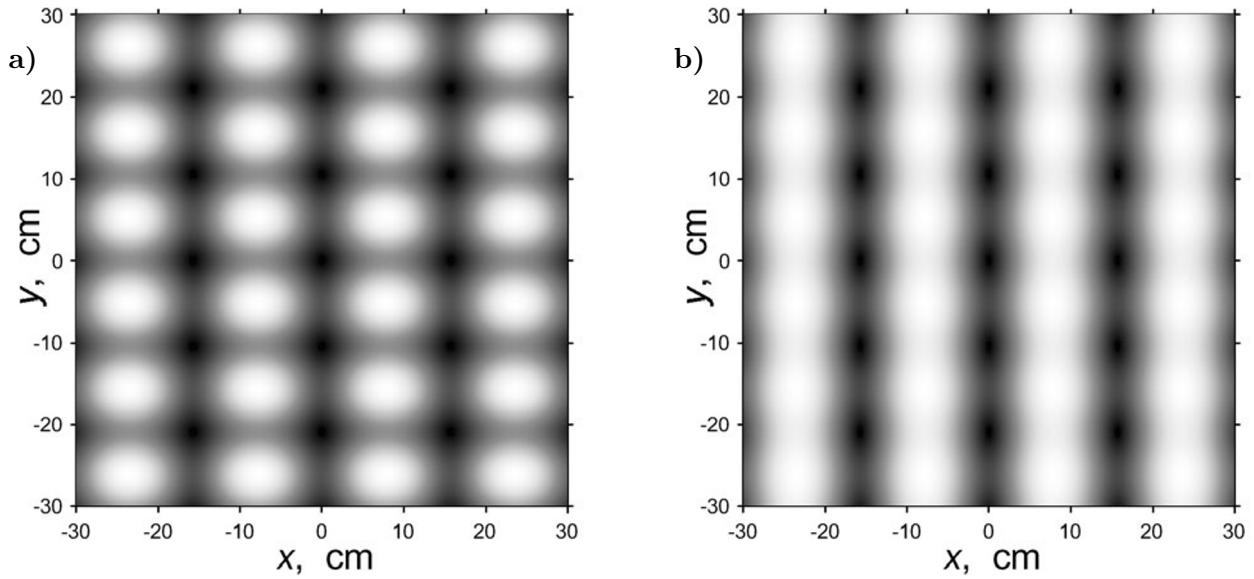


Fig. 6. Normalized intensity of a PC-sin beam with $\sigma_0 = 4$ mm, $a = 20$, and $b = 20$ in non-Kolmogorov turbulence. Here, $L = 200$ m (a) and $L = 1000$ m (b).

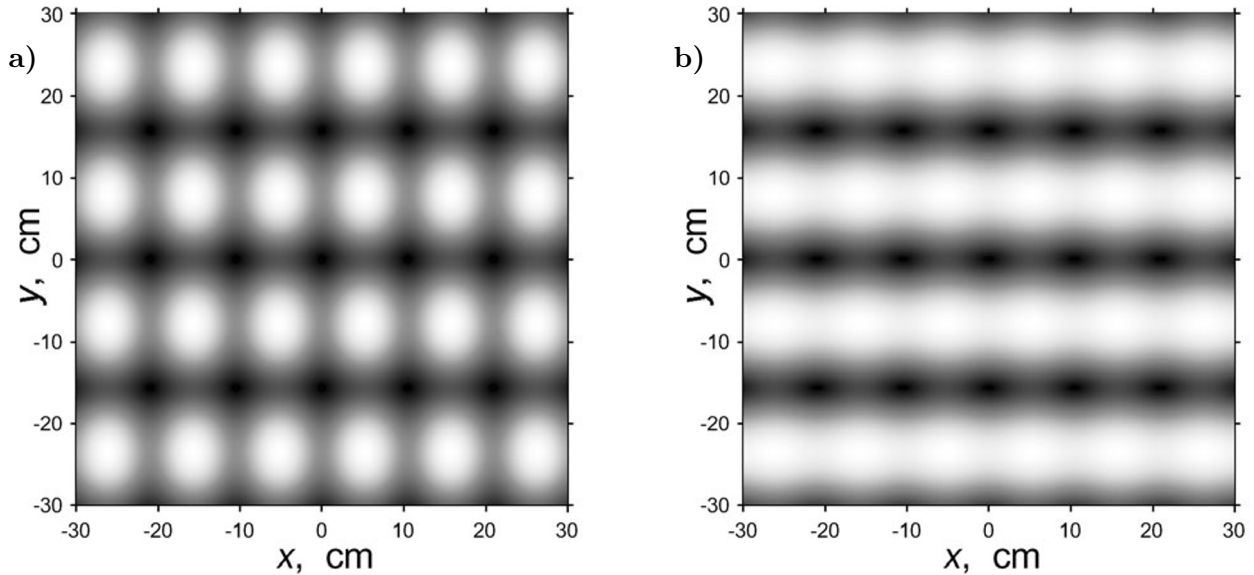


Fig. 7. Normalized intensity of a PC-sin beam with $\sigma_0 = 4$ mm, $a = 30$, and $b = 20$ in non-Kolmogorov turbulence. Here, $L = 200$ m (a) and $L = 1000$ m (b).

quickly with a smaller coherence length σ_0 and stronger turbulence.

In Figs. 6 and 7, we illustrate the intensity profile of the PC-sin beam with different a and b values in non-Kolmogorov turbulence. In Fig. 6, one can see that the symmetry profile of the PC-sin beam with $a = 20$ and $b = 30$ is destroyed during the propagation. The beamlets of the PC-sin beam overlap along the y direction, when $a < b$, are shown in Fig. 6, where the PC-sin beam has a similar sheet profile along the y direction. When $a > b$ (Fig. 7), the sheet profile of the PC-sin beam at $L = 1000$ m becomes oriented along the x direction. The results demonstrate that the symmetry profile of a beam is destroyed,

when $a \neq b$, and the array beam profile becomes a sheet profile.

4. Conclusions

In summary, we introduced the expression of the PC-sin beam and derived the CSD of the PC-sin beam propagating in non-Kolmogorov turbulence. We calculated and analyzed the intensity profile of the PC-sin beam in non-Kolmogorov turbulence. We found that the array beam shape was destroyed under a smaller σ_0 and non-Kolmogorov turbulence. We state that a PC-sin beam with smaller σ_0 or propagation in stronger turbulence will lose the beam array profile faster. It is also seen that the intensity profile of such a beam in non-Kolmogorov turbulence can evolve into a sheet profile, when different values of a and b are set. The phenomenon that the sine beam evolves into Gaussian-like beam may be useful for FSO communications.

Acknowledgments

This work was supported by the National Natural Science Foundation of China under Grants Nos. 11604038, 11404048, and 11875096.

References

1. H. T. Eyyuboglu, Y. Baykal, and E. Sermutlu, *Opt. Commun.*, **265**, 399 (2006).
2. Y. Cai, *J. Opt. A*, **8**, 537 (2006).
3. P. Zhou, X. Wang, Y. Ma, et al., *J. Opt.*, **12**, 015409 (2010).
4. Y. Liu, K. Zhang, Z. Chen, et al., *Optik*, **181**, 571 (2019).
5. Y.-Q. Li, W.-Y. Zhu, and X.-M. Qian, *Chin. Phys. B*, **30**, 034201 (2021).
6. F. Wang, X. L. Liu, and Y. J. Cai, *Prog. Electromagn. Res.*, **150**, 123 (2015).
7. Y. J. Cai, Q. Lin, Y. Baykal, et al., *Opt. Commun.*, **278**, 157 (2007).
8. H. Y. Wang and X. Y. Li, *Optik*, **122**, 2129 (2011).
9. Q. Suo, Y. Han, and Z. Cui, *Opt. Laser Technol.*, **123**, 105940 (2020).
10. Z. Hricha, M. Lazrek, M. E. Halba, et al., *Opt. Quantum Electron.*, **54**, 719 (2022).
11. Y. H. Chen, F. Wang, and Y. J. Cai, *Adv. Phys.-X*, **7**, 2009742 (2022).
12. H. F. Xu, Z. Zhang, J. Qu, et al., *Opt. Express*, **22**, 22479 (2014).
13. X. Wang, M. Yao, X. Yi, et al., *Opt. Laser Technol.*, **87**, 99 (2017).
14. Z.-Z. Song, Z.-J. Liu, K.-Y. Zhou, et al., *Chin. Phys. B*, **26**, 024201 (2017).
15. H. F. Xu, H. W. Wu, H. J. Chen, et al., *J. Mod. Opt.*, **66**, 208 (2019).
16. D. Liu, Y. Wang, H. Zhong, et al., *Opt. Laser Technol.*, **119**, 105604 (2019).
17. J. Zhao, G. Wang, Y. Yin, et al., *Optik*, **241**, 167237 (2021).
18. H. Zhang, Z. Cui, Y. Han, et al., *Front. Phys.*, **9**, 650537 (2021).
19. L. Liu, H. Wang, L. Liu, et al., *Front. Phys.*, **10**, 847649 (2022).
20. B. Sun, H. Lü, D. Wu, et al., *Photonics*, **8**, 82 (2021).
21. Y. H. Mao, Z. R. Mei, and J. G. Gu, *Opt. Laser Technol.*, **86**, 14 (2016).
22. Y. P. Huang, A. P. Zeng, Z. H. Gao, et al., *Opt. Lett.*, **40**, 1619 (2015).
23. Z. Z. Song, Z. J. Liu, K. Y. Zhou, et al., *J. Opt.*, **18**, 105601 (2016).
24. D. Razzaghi, F. Hajiesmaeilbaigi, and M. Alavinejad, *Optik*, **124**, 2135 (2013).
25. D. Liu, Y. Wang, and H. Zhong, *Opt. Laser Technol.*, **106**, 495 (2018).
26. Y. Huang, Y. S. Yuan, X. L. Liu, et al., *Appl. Sci.*, **8**, 2476 (2018).

27. L. Lu, Z. Wang, and Y. Cai, *Opt. Express*, **29**, 16833 (2021).
28. X. Ma, D. Liu, Y. Wang, et al., *Appl. Sci.*, **10**, 450 (2020).
29. Y. Yan, G. Wang, Y. Yin, et al., *Heliyon*, **8**, e11295 (2022).
30. G. Huang, G. Lv, Y. Fan, et al., *Opt. Laser Technol.*, **146**, 107528 (2022).
31. M. Wang, T. Kane, X. Yuan, et al., *Opt. Express*, **26**, 32130 (2018).
32. Y. Yuan, J. Zhang, J. Dang, et al., *Opt. Express*, **30**, 5634 (2022).
33. M. Bayraktar, *Microw. Opt. Technol. Lett.*, **64**, 1858 (2022).
34. Y. Li and E. Wolf, *Opt. Lett.*, **7**, 256 (1982).
35. F. Gori, M. Santarsiero, G. Piquero, et al., *J. Opt. A*, **3**, 1 (2001).
36. H. Roychowdhury and O. Korotkova, *Opt. Commun.*, **249**, 379 (2005).
37. H. Tang and B. L. Ou, *Opt. Laser Technol.*, **43**, 1442 (2011).
38. G. Q. Zhou, *Opt. Express*, **19**, 24699 (2011).
39. Y. Zhang, T. Hou, Q. Chang, et al., *IEEE Photonics J.*, **12**, 1 (2020).